AB INITIO DENSITY STUDY OF N AND O COADSORPTION ON Pt(100) AND Pt(111)

A Dissertation

Submitted to the African University of Science and Technology

in partial fulfillment of the requirement for

MASTER OF SCIENCE DEGREE OF CONDENSED MATTER PHYSICS

By

Obodo, Tobechukwu Joshua

Supervisors:

Reg. no: 40034

Prof. Sandro Scandolo

and

Dr. Prasenjit Ghosh

African University of Science and Technology, Abuja.

Nigeria.

November 13, 2009

Dedication

This work is dedicated to 'The grand energy minimizer': Almighty God

Acknowledgment

I would like to express my sincere gratitude to my supervisor Prof. Sandro Scandolo and co-supervisor Dr. Prasenjit Ghosh for their all suggestions, inspirations and guidance in the completion of this work, their assistance and valuable suggestions at all times has been of immense value. I would like to express my immense gratitude to Dr. Karl Voltaire for his fatherly advice and his guidance towards the search for 'the next African Einstein'. Also to Dr. Boubou Cisse, Zainab El-Rufai, and Olajide Babatunde Abiodun for indeletable seed planted in me.

Special thanks and gratitude also goes to our respected teachers Prof. Douglas Buttery, Prof. Charles Chidume, Prof. Dimo Uzunov, Dr. Bashir and Prof.(Mrs.) R. U Osuji for their valuable suggestions and help through out this programme. I would also like to express my sincere gratitude to the ICTP IT department for their great help with computer related problems.

I would also like to appreciate my respected parents Chief and Mrs. C. N. Obodo and my lovely siblings; Obodo Sabinus, Obodo Kingsley, Nnenna, Chinyere, Nnamdi, Chidiebere and Sopuluchukwu, my cousins; Amalu Emeka, Azubuike, Obodo Salome, Ifeoma, for their encouragement and support during my study. I express my sincere gratitude to my friends Abah Obinna, Ogbuu Okechukwu, Elvis Esharegharan, Onuh Haruna, Ekuma Chinedu, Eze

Ifeoma, Onah Ekene, Ahia Chinedu, Ogbene Alexis, Ojemba Sebastine and ... your love and encouragement has been like a life support

I am ever grateful and indebted to the African University of Science and Technology, Abuja and the Abdus Salam ICTP, for its warm hospitality and financial support without which I would not have been able to access this opportunity.

Finally, I would like to acknowledge my classmates; Akosa Collins, Igumbor Emmanuel, and Adjokatse Sampson who helped in making the environment conducive for learning by sharing their feelings and knowledge during the course of this work.

Obodo, Tobechukwu Joshua

Contents

List of Tables

List of Figures

Abstract

We have used *ab initio* density functional theory to study the coadsorption of N and O on Pt(100) and Pt(111) surfaces. Our calculations show that on Pt(100) the most favourable site is the hollow site for N and the bridge site for O, while for Pt(111) there are different possible N and O coadsorption geometries. On both surfaces the interaction between N and O is repulsive in nature.

Chapter 1

Introduction

Unlike other reagents that participate in the chemical reaction, a catalyst is not consumed by the reaction itself but alters the rate of chemical reaction. The catalyst may participate in multiple chemical transformations.

Generally, catalysts are transition metals which have different number of d-electrons which play an important role in the performance of the catalyst. Heterogeneous catalysts are those which are in different phases than the reactants. Most heterogeneous catalysts are in solid phase while the reactants and products are in liquid or in gaseous phase. Diverse mechanisms for reactions on surfaces are known, depending on how the adsorption takes place (Langmuir-Hinshelwood and Eley-Rideal)[25].

Intensive studies on the adsorption of small molecules on metallic surfaces have been carried out due to their potential applications in several technological proceses, such as heterogeneous catalysis, corrosion, lasers and gas sensors [1]. Automotive exhausts contain several noxious gases, such as CO and NO, which need to be converted to less harmful products (e.g., CO oxidized to CO_2 , and NO reduced to N_2) before they are released into the atmosphere. Technologically, NO is involved in many industrial processes, such as ammonia oxidation (NO is oxidized into HNO3) and emission control (NO is reduced to N2). The surfaces of metals like Pt, Ir and Rh have been found to be good catalysts for such reactions. A better understanding of the catalytic activity of these surfaces could lead to the development of cheaper and better catalysts, and these reactions have therefore been the subject of extensive experimental and theoretical studies [2] In a catalytic process the overall reaction usually consists of a series of elementary steps. These includes adsorption of the reactants on the surface of the catalyst, diffusion on the surface, breaking of some reactant bonds and formation of new ones to form the product molecules, which is eventually desorbed from the surface.

The rate of a chemical reaction depends on the height of the potential barrier separating two minima of potential energy (of the reactants and the products of a reaction). To calculate reaction barriers several techniques exist, but the Nudged elastic band method is the most widely used one to determine the reaction pathways when both the initial and final states are known.

This thesis involves the study of the coadsorption energy of N and O which is the final state of the NO dissociation reaction.(NO dissociation being the rate limiting step of the conversion of NO to less harmful product), for which platinium is used as a catalyst.

The rest of the thesis is divided into different chapters. The second chapter provides a brief introduction of density functional theory. In chapter three, we describe in brief the methodology used in the calculations and present the results of the tests performed by us to determine different parameters of the calculation. Our main results are presented in chapter four,while we summarize and conclude our work in chapter five.

Chapter 2

BACKGROUND LITERATURE

2.1 DENSITY FUNCTIONAL THEORY

Density Functional theory (DFT) has long been the mainstay of electronic structure calculations in solid-state physics. This is because approximate functionals were shown to provide a useful balance between accuracy and computational cost. This allowed much larger systems to be treated than by traditional *ab initio* methods, while retaining much of their accuracy. Nowadays, traditional wavefunction methods, either variational or perturbative, can be applied to find highly accurate results on smaller systems, providing benchmarks for developing density functionals, which can then be applied to much larger systems. Lets consider a system of M ions and N electrons. To know the microscopic properties we need to sovle the Schrodinger equation which is

$$H\Psi = E\Psi$$

where Ψ is the wave function of the system and H is the Hamiltonian acting on it, and E is the energy eigenvalues. The Hamiltonian for such a system is given by;

$$H = \sum_{i=1}^{N}(-\frac{1}{2}\nabla_{r_i}^2) + \sum_{j=1}^{N}(-\frac{1}{2}\nabla_{R_j}^2) - \sum_{i=1}^{N}\sum_{j=1}^{M}(\frac{Z_j}{|r_i - R_j|}) + \sum_{i<j}\frac{1}{r_{ij}} + \sum_{i<j}\frac{Z_i Z_j}{R_{ij}} \tag{2.1}$$

where Z_i is the charge on the ion. Note that atomic units (e^2=m_e=h=1) have been used.

The first approximation which can be done is the separation of the ionic degrees of freedom from the electronic ones. This is the so called Born-Oppenheimer (or adiabatic) approximation. Ions are much heavier than electrons and the electrons follow adiabatically the ionic movements, remaining close to their instantaneous ground state. In this way the ions act as external potential sources for the electronic problem, which therefore depends only parametrically on the ionic positions,

$$(H(R) - E(R))\psi(r_i, R) = 0 \tag{2.2}$$

$$H = \sum_{i=1}^{N}(-\frac{1}{2}\nabla_{r_i}^2) - \sum_{i=1}^{N}\sum_{j=1}^{M}(\frac{Z_j}{|r_i - R_j|}) + \sum_{i<j}\frac{1}{r_{ij}} \tag{2.3}$$

where, ψ is electronic wave function. Once the electronic problem is solved (ideally for each ionic position), the dynamics of the ions can be studied using the electronic energy E(R) as effective potential. Usually ions are heavy enough to be treated as classical particles, which is therefore a further reasonable approximation. It is still difficult to solve because of the presence of the many-body wave function $\psi(r_i, R)$. Besides such a wave function based approach, another formalism has been developed in the last three decades:it is the Density funcitonal theory(DFT)[2].

The idea of DFT was originally introduced by Hohenberg and Kohn(HK). They showed that the external potential is a function of the electronic ground state(GS) density given by $n(r) =< \psi_i|\hat{n}(r)|\psi_j >$, for which ψ is the ground state wave function and $\hat{n}(r)$ is the density operator.
Mathematically, the energy of the system can be expressed as a functional of density [4]

$$E(n) = F_{HK}[n] + \int V_{ext}(n)\hat{n}(r)dr \tag{2.4}$$

where V_{ext} is the external potential due to ion-electron interaction and the $F_{HK}[n]$ is a universal functional because it does not depend on the external potential, but it is a function of the sum of the kinetic and potential energy operators of the electron-electron interaction .

$$F_{HK}[n] =< \psi[n]|T + V|\phi[n] > \tag{2.5}$$

HK showed that the GS density of the system is the one which minimizes the $E[n]$, and also the minimum $E[n]$ is the GS energy E_0. The exact form of the functional is unkown, but it is know to be a function of density and this simplifies it. One year after HK paper, Kohn and Sham (KS) [4] where able to show a practical means to solve the problem. The idea is to consider an auxillary non-interacting system whose density is the same as the one of the real system. The wave form of the non-interacting system is known as the Kohn Sham Orbital ($\phi_i(r)$) and they obey the orthogonality condition.

$$\int \phi_i^*(r)\phi_j(r)dr = \delta_{ij}$$

The electron density is defined as

$$n(r) = \sum_i |\phi_i(r)|^2$$

Considering the energy funcitonal for which $T_0[n]$ is the GS kinetic energy of the auxiliary non-interacting system, $E_H[n]$ is the replusive electrostatic energy of the classical charge distribution $n(r)$ and $E_{xc}[n]$ is the exchange-correlation (XC) energy and applying variational principle to minimize the energy functional and using the orthogonality condition as a constraint, one finds a set of one-particle Schrodinger equaitons;

$$[\frac{1}{2}\nabla^2 + V_{KS}]\phi_i(r) = \varepsilon_i\phi_i(r) \tag{2.6}$$

where the Kohn-Sham (KS) potential is given by

$$\begin{aligned} V_{KS} &= V_{ext}(r) + \int \frac{n(r')}{|r-r'|}dr' + V_{xc}(r); && (2.7) \\ V_{xc} &= \frac{\delta E_{xc}[n]}{\delta n(r)} && (2.8) \\ &and \\ n(r) &= \sum_{i=1}^{\infty} f(\epsilon_i - \epsilon_F)|\phi_i(r)|^2 && (2.9) \end{aligned}$$

These equations are the famous KS equation which must be solved self-consistently since V_{KS} is a functional of the electron density and $f(\alpha)$ is the Fermi-Dirac distribution for $\alpha = \epsilon_i - \epsilon_F$ where the Fermi energy is ϵ_F.

Upon the achievement of convergence the electronic energy of the system is given by

$$E = \sum_{i=1}^{N} f(\epsilon_i - \epsilon_F)\epsilon_i - \frac{1}{2}\int \frac{n(r)n(r')}{|r-r'|}dr + E_{xc}[n] - \int V_{xc}n(r)dr + E_{ion} \tag{2.10}$$

where E_{ion} is the ionic electrostatic repulsion energy. This would be the exact electronic ground state energy of the system if the exact $E_{xc}[n]$ is known [12].

2.1.1 Local Density Approximation

Prior to this approximation, the mapping of the interacting electron system onto the noninteracting system, was of formal interest only, until a way to approximate the correlation potential was introduced. One way is to consider the correlation energy per electron $\epsilon_c(n)$ in the homogeneous electron gas of density. This energy can be computed with relatively high precision using Monte Carlo methods. Under this approximation the correlation energy can be written as $\int \epsilon_c(n(r))n(r)dr$. However, this does not yield in practice good energy as enough results and is thus seldom used. A more successful ways was devised by Kohn and Sham [13] and displayed in an analytical form [15] for both the exchange and correlation energy per electron in the homogeneous gas,

$$E_{xc}^{LDA}[n] = \int \epsilon_{xc}(n(r))n(r)dr - E_x[n] \tag{2.11}$$

This approximation is called the local density approximation (LDA)[4]. The functional of (2.11) leads to the following LDA approximation for the energy functional:

$$E_{xc}^{LDA}[n] = T_0[n] + \int v(r)n(r)dr + \int \epsilon_{xc}(n(r))n(r)dr \tag{2.12}$$

This approach is highly successful and is considered in DFT as the basis for most of the developments of other functionals.

2.1.2 Generalized Gradient Approximation

As the LDA approximates the energy of the true density by the energy of a local constant density, it fails in situations where the density undergoes rapid changes such as in molecules. An improvement to this can be made by considering the gradient of the electron density, the so-called Generalized Gradient Approximation (GGA). Symbolically this can be written as

$$E_{xc}^{GGA} = E_{xc}^{GGA}[\rho(r), \nabla\rho(r)] \tag{2.13}$$

Where $\nabla\rho(r)$ is the gradient of density as a function of position.
This can lead to a large improvement over LDA results with accuracy approaching that of correlated wavefunction methods. A commonly used functional is the PW91 functional, due to Perdew and Yang [16] [17].

2.2 INFINITE PERIODIC SYSTEM

It is clear that only system with finite number of atoms can be studied in practice. This implies that the eigenvalue and eigenstates of a system in 2.6 has to be found. However, if the system is a periodic solid, then the KS potential is a periodic funciton of the lattice.

$$V_{KS}(r+R) = V_{KS}(r); \forall R \in \textbf{Bravias Lattice} \tag{2.14}$$

The solution of the (2.6) can be written in Bloch form,

$$\phi_i(r) = \phi_{nk}(r) = e^{ik.r}u_{nk}(r) \tag{2.15}$$

and n is the band index. Subsitituting eqn2.15 in eqn.2.6

$$\{-(\nabla + ik)^2 + V_H(r) + V_{xc}(r) + V_{ext}(r)\}u_{nk} = \epsilon_{nk}u_{nk} \tag{2.16}$$

In calculating the electronic properties of the system; such as the total energy, and the ionic forces, integrations in the whole BZ are required. This implies that infinite solutions of the eqn.2.16 is required, but this is taken care of by the consequences of Bloch's theorem. The quality of the approximation can be checked by increasing the number of k-points logically. The development of k-points has been from Baldereschi [11] to Chadi and Cohen [23] and Monkhorst and Pack [18]. For smooth functions a small number of k-points is required but for occupation functions like that of metal, large k-points is required to aid faster convergence of the solution. Also, to speed up the convergence with respect to k-point mesh, Fu and Ho [24] introduce a way of introducing an appropriate Fermi-Dirac like behaviour. Though, this introduces an error in the integrals that depend on the electronic temperature and smearing functions, these errors can be controlled.

2.3 PSEUDOPOTENTIAL

The pseudopotential formalism grew out of the Orthogonalized Plane Wave(OPW) method [7], in which valence wave functions were expanded in a set of plane waves(PW) which are orthogonalized to all of the core wavefunctions. In solving the Schordinger wave equation for condensed aggregates of atoms, space is being divided into two regions with quite different properties. The core region comprises typically of tightly bound core electrons which respond very little to presence of neighbouring atoms, while the remaining volume contains the valence electron density which is invloved in the bonding together of the atoms.

$$|OPW, K >= |PW, k > - \sum_{c}^{core} |\psi_c >< \psi_c|PW, K > \tag{2.17}$$

The construction of a pseudopotential can be demostrated in terms of the exact core and valence states $|psi_c >$ and $psi_v >$, which satisfies its corresponding Schrodinger equation.

$$H\psi_i = E\psi_i,\ for\ i = c{,}v \tag{2.18}$$

Subtracting the core orthogonality smoothens the valence state in the core region leading us to pseudostates $|\phi_v>$ given by;

$$|\phi_v >= |\psi_v > + \sum_c E_c|\psi_c >< \psi_c|\phi_v > \tag{2.19}$$

Acting the Hamiltonian on the wave funciton in 2.19, we get

$$\begin{aligned} H|\phi_v > &= E_v|\psi_v > + \sum_c E_c|\psi_c >< \psi_c|\phi_v > \\ &= E_v|\phi_v > + \sum_c (E_c - E_v)|\psi_c >< \phi_c|\phi_v > \end{aligned} \tag{2.20}$$

Eqn.2.20 can be expressed as

$$\{H + \sum_c (E_v - E_c)|\psi_c >< \phi_c|\}|\phi_v >= E_v|\phi_v > \tag{2.21}$$

Eqn.(2.21), shows that the valence pseudo-states $|\phi_v>$ satisfies the Schrodinger equation with an energy dependent pseudo Hamiltonian.

$$H^{ps} = H + \sum_c (E_v - E_c)|\psi_c >< \phi_c| \tag{2.22}$$

This implies that, we have compromised the orthogonality wiggles at the expense of introducing energy-dependent, non-local repulsive potential. The psuedopotenial is sketched in Fig.2.1

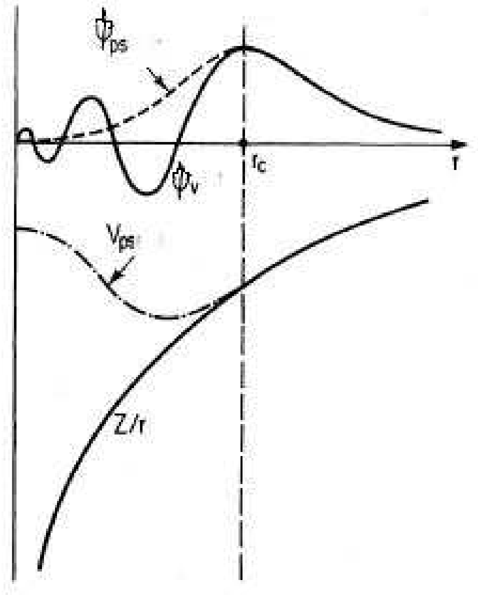

Figure 2.1: Schematic representation of the pseudopotential method. the electron potential $-Z/r$ orbital ϕ are altered to the pseudopotenial V_{ps} and pseudo -orbital ϕ^{ps} inside the core of radius r_c

For many atoms system, the Phillips-Kleiman [9], potential is found to be good enough, because it makes the solid behave like an electron gas, which implies a weak potential, for this reason it is worth the additional complexity

$$V^{pk} = V + \sum_{c}(E - E_c)|\psi_c >< \phi_c| \tag{2.23}$$

2.3.1 Pseudopotential Approximation

Due to the localization of the core electrons and to the rapid oscillations in the core region of the wave-functions which describe the valence electrons, the number of PWs needed, even for a simple calculation, is huge. We need approximations to avoid this problem. The first idea is to disregard the core electrons because they do not participate in the chemical properties of matter, at least until their binding energy is much higher than the energy involved in the chemical properties one wants to study. So one freezes them around the nuclei and redefines the system as if it was formed by ions plus valence electrons. We are left with the second problem, how to deal with the oscillations in the core region of the valence wave-functions, due to the orthogonalization to the core wave functions. The solution to this is the introduction of a pseudopotential (PP) which substitutes the ionic Coulomb potential in such a way that the valence pseudo eigenvalues are the same as the all electron (AE) ones and the pseudo wave functions coincide with the AE ones beyond a fixed core radius on, and are as smooth as possible below the core radius, with the only constraint to be normalized (norm-conserving (NC) pseudo-potentials). An ionic potential, valence wave function and corresponding pseudopotential and pseudo wave function are illustrated in Fig.2.1 The figure shows that pseudo wave function and all electron wave function(AE) and corresponding pseudopotential and ionic potential are identical outside the cutoff radius r_c . Near the core region there is rapid oscillation of AE wave function while pseudo wave function is smooth. To satisfy this requirements the PP usually must be angular momentum dependent, i.e. pseudo-wave-functions corresponding to different angular momenta are eigenfunctions of different potentials. However, the long range behaviour of these different potentials must resemble the true one, because above the core radius the pseudo-wave-functions are identical to the AE ones. This means that the difference must be confined in the core region and then the PP can be written in the following form [20]

$$V_s^{sl}(r, r') = V_s^{loc}\delta(r - r') + \sum_{l=0}^{l_{max}} V_{s,l}^{nl}(r) P_l(\hat{r}, \hat{r}')\delta(r - r') \tag{2.24}$$

where $V_s^{loc}(r)$ is a local, long range part and approaches the AE potential above a cutoff radius r_c^{loc} , and $V_{s,l}^{nl}(r)$ are the non-local short range angular momentum dependent part, the index s refers to the atom, the superscript sl emphasizes the semi-locality (non local in angular momentum but local in r) and P_l is the projector onto the angular momentum l,

$$P_l(\hat{r}, \hat{r}') = \sum_{m=-l}^{l} Y_{l,m}(\theta', \phi') \tag{2.25}$$

with the $Y_{l,m}$s the spherical harmonics. The quality of the PP depends on transfer- ability properties, i.e. the capability to reproduce the AE results over a wide range of electronic configuration.

2.3.2 Ultra-Soft (Vanderbilt) pseudopotentials

The requirement of norm conservation for the pseudo-wave-functions can be a limiting factor for numerical calculations when also the valence electrons are very localized around the nuclei. For the first row elements,like carbon and more so for nitrogen, oxygen, and for transition metals, where the d-electrons are as localized as shallow core states but have an extraction energy which is comparable to valence energies, and for this reason cannot be excluded from the calculation. If this is the case the utilization of NC pseudopotentials requires huge PWs basis sets to achieve an acceptable accuracy. Vanderbilt 1990 [10] introduced a generalized formalism which made it possible to remove the norm conservation constraint. In this way one can construct much smoother pseudo wave functions, with the only constraint of matching the AE ones and above a fixed core radius The price to pay for having so smooth pseudo-wave-functions is the introduction of a new generalized formalism. Due to the fact that the pseudo wave functions are no more normalized, the charge density has to be restored by adding an augmentation part.

$$n(r) = \sum_{n,k} |\phi_{nk}(r)|^2 + n_{aug}(r) \tag{2.26}$$

and the KS equation has the new generalized form:

$$H_{KS}|i >= \varepsilon_i S|i > \tag{2.27}$$

where S is a non-local overlap operator.

2.3.3 Forces

One very essential ingredient in optimizing geometrical structures or studying the dynamical evolution of systems is the force acting on the atoms. The ionic mass becomes important, of which the forces acting on the masses are derivates of the energy with respect to their displacements. Applying the

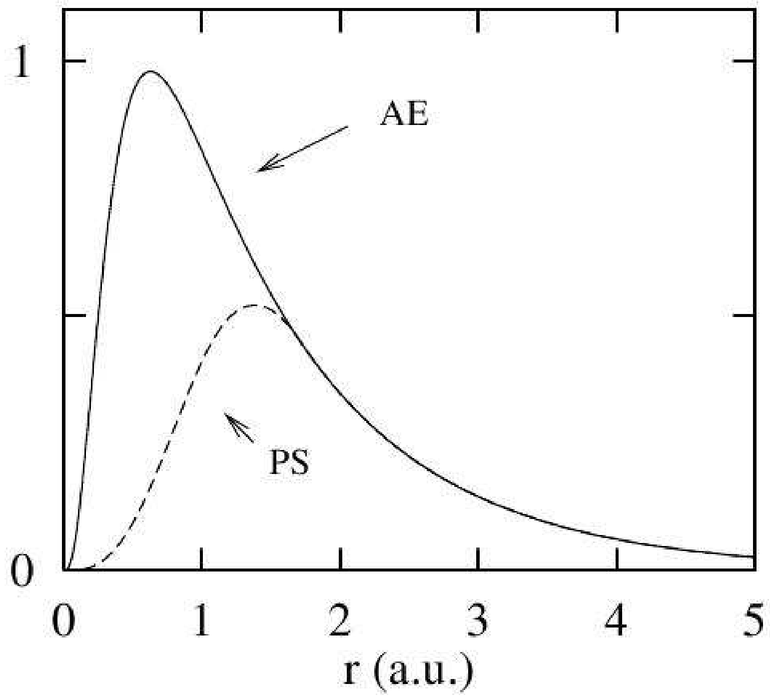

Figure 2.2: All-electron (solid) and Ultra-Soft pseudo (dashed) radial wave-functions of the 3d orbital of nickel. rc = 1 : 75 a.u

Hellman-Feynman theorem [19],[21]. In case of forces, λ is the collection of the ionic positions. The energy derivative with respect to λ is given as

$$\frac{\partial E}{\partial \lambda} = \int n_\lambda \frac{\partial V}{\partial \lambda} \tag{2.28}$$

With the knowledge of the actual density, then the total energy and force acting on the atoms can be calculated via self-consistent calculation.

2.4 Surface Modelling

A surface is a created from bulk by cutting along certain high symmetry directions. For a surface, its coordination number and periodicity varies from that of its bulk. For simulations, surfaces are either created via slab method or cluster method. For the purpose of this work we will be using the slab method. In this method, the periodicity along the direction perpendicular to the surface is broken. This is shown in Fig. 2.3

In order to describe the properties of a surface, one must make sure that the slab used to mimic the surface is sufficiently thick. Along the direction perpendicular to the surface the distance between the periodic images should be sufficiently large in order to avoid any spurious interaction between them.

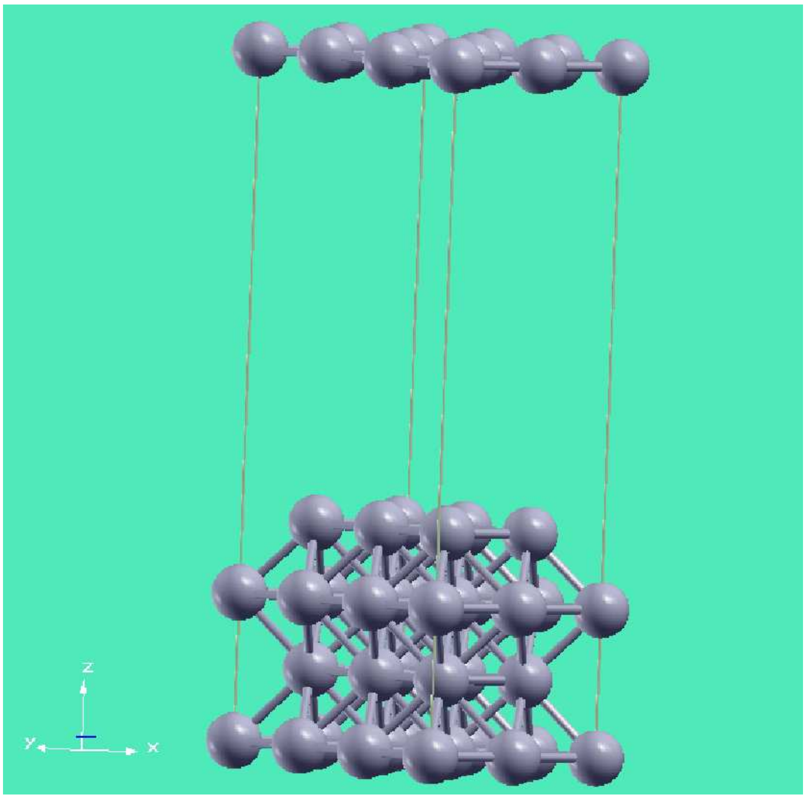

Figure 2.3: Demostration of broken symmetry along the z-direction

Chapter 3

Methodology and Test Calculations

3.1 Methodology

All calculations are carried out using the pw.x code of the Quantum Espresso package [22] which is an implementation of DFT [4]. The Perdew-Burke Ernzerhof(PBE) [15] based generalized gradient approximation (GGA) was used for the exchange-correlation functional.The wavefunction have been expanded in a plane wave basis set. The ionic cores are described with ultrasoft pseudopotentials with scalar-relativistic calculations as implemented in the PWSCF code [8]. The Brillouin zone is sampled with the Monkhorst-Pack k-point mesh.

3.2 Test Calculations

The results of the calculations depend on correct choice of different parameters like wave function cutoff (which determines the size of the basis set), augmentated charge density (which is introduced due to the use of ultrasoft pseudopotential), choice of k-point mesh, etc. In the following section, we present the results of some test calculations to determine the suitable parameters used.

3.2.1 Determination of Augumented Charge Density cutoff (E_{cutrho})

In order to determine the cut off for the augumented charge density (E_{cutrho}), we calculated the total energy of bulk Pt using the experimental lattice parameter as a function of E_{cutrho}.

The result is shown in Fig. 3.1. From the figure we find that beyond 320Ry, the changes in total energy are of the order of 1meV. Therefore for our calculation we have used 320Ry as the cutoff for the augumented charge density.

3.2.2 Determination of plane wave cut off (E_{cutwfc})

The bulk lattice parameter was varied for different values of E_{cutwfc} fixing the value of E_{cutrho} to the determined value of 320Ry. Plot of the total energy as a function of lattice parameter for different values of E_{cutwfc} is shown in Fig. 3.2 and it was observed that total energy for bulk platinium converges within 1meV when we use E_{cutwfc} = 50Ry. It is observed that converges

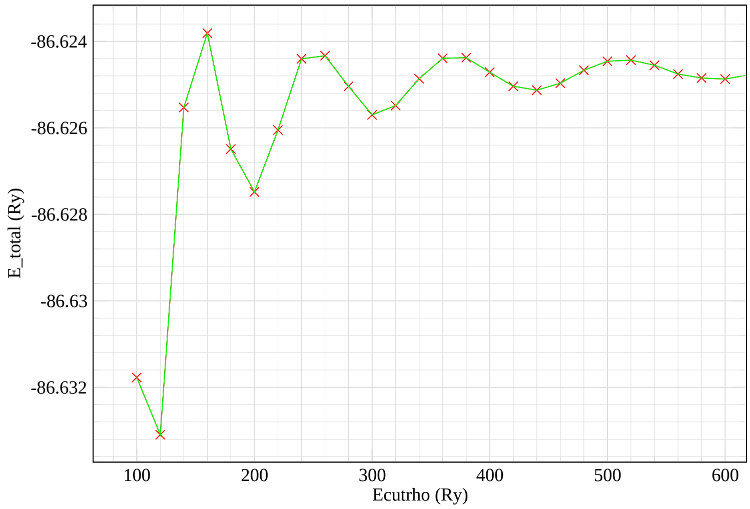

Figure 3.1: Convergence of 'Ecutwfc' with respect to the total energy for Platinium

faster as a function of E_{cutwfc} rather than the total energy, this is because we are intrested in the adsorption energies which is as a result of changes in energy.

In order to save computational time, we have also looked into the convergence of the difference in energy (δE) between two values of lattice parameter (7.40Å and 7.48Å) with respect to E_{cutwfc}. The result is shown in Fig.3.3. We find that the change in δE is of the order of 1meV when E_{cutwfc} = 35Ry. Therefore, for the rest of the calculations we use the value of E_{cutwfc} as 35Ry.

3.2.3 k-point mesh

The Brillouin zone is sampled with Monkhorst-Pack k-point mesh, and the value of a mesh which is sufficient enough for our calculation was determined

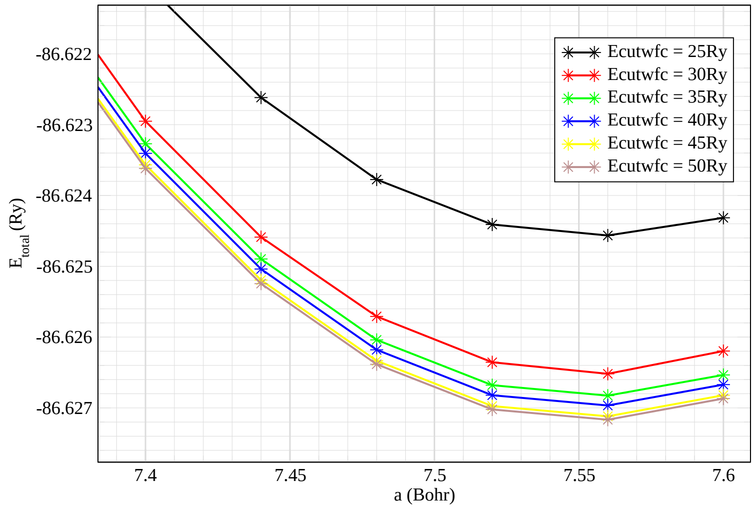

Figure 3.2: E_{total}(Ry) vs. lattice parameter, a (Bohr) for Pt

from the convergence point of the plot of varying k-point as a function total energy as a function of the number of k-point as shown in Fig.3.4.

3.2.4 Test for Pseudopotential

In order to test the pseudopotentials used in the calculations, we calculate the bulk lattice parameter of platinum using the above mentioned values of computational parameters. We determine the lattice constant to be 4.00Å which is in excellent agreement with previously calculated values of 4.00 Å [26] and is in reasonably good agreement with experimentally measured value value of 3.92 Å [27].

For N and O we have used ultrasoft pseudopotentials with the same values of E_{cutwfc} and E_{cutrho} as that for Pt. In order to test the pseudopotentials, we have studied the atomization energies and the bond-length of N_2, O_2, and

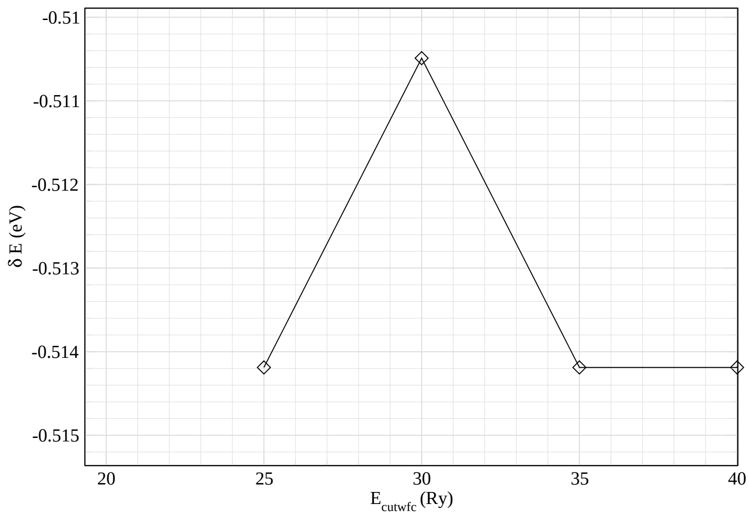

Figure 3.3: δE(eV) vs. Ecutwfc(Ry) for Pt

NO in gas phase. The molecules have been kept in a large cubic box of size 30 bohr. The integratins over the BZ have been performed using the gamma point only. The atomization energies were calculated using

$$\Delta E = E_{AB} - E_A + E_B \tag{3.1}$$

where E_{AB}, E_A and E_B are the total energies of the molecule AB, atom A and atom B respectively. For the case of NO, A is N and B is O while for N_2 (O_2), A = B = N (O).

The binding energies and bond lengths of these molecules have been compared with experimental values and previous calculations and the results are presented in Table 3.1.

For N_2, O_2 and NO we obtain bondlengths of 1.11, 1.21 and 1.17 Å respectively. The atomization energies are -9.85, -6.66 and -7.24eV for N_2, O_2 and NO respectively. For all the three molecules our results are in reasonably

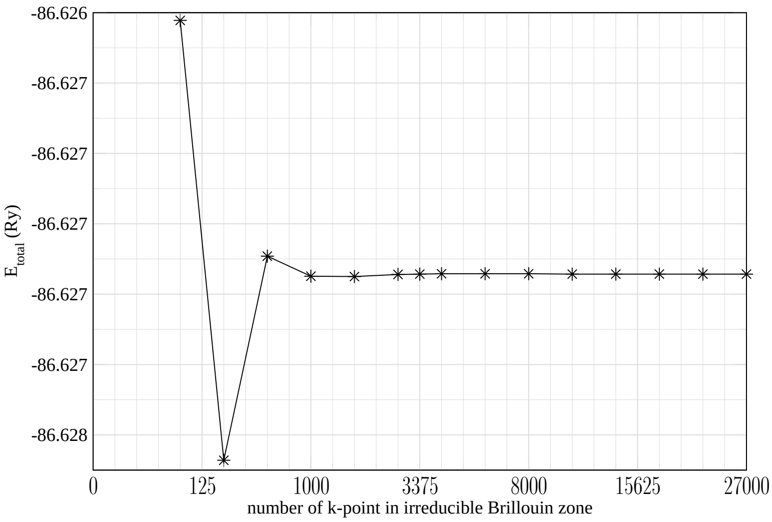

Figure 3.4: Test of convergence of E_{total} as a function of number of k-points in Irreducible Brillouin zone

good agreement with experimental and previous theoretical calculations.

Table 3.1: The bond length and the binding energies of N_2, O_2 and NO.

	$E_{ad}(eV)$			d_{A-B} Å		
molecule	cal.	previous th. cal.	exp.	cal.	previous th. cal	exp.
N_2	-9.85	-10.54[16]	-9.93 [16]	1.11	1.11	–
O_2	-6.66	-6.24 [16]	-5.25 [16]	1.24	1.21	–
NO	-7.24	-7.13 [2]	-6.63[16]	1.17	1.17 [31]	1.15 [31]

Chapter 4

RESULTS

In order to study N and O coadsorption on Pt(100) and Pt(111), the surfaces have been modeled with four layer thick slab of which only the top two layers were relaxed. To study the clean surface, we have used a (1x1) surface unit cell, while to study the N and O coadsorption we have used a (2x3) surface unit cell. The brillouin zone is sampled with a (12 x 12 x 1) k point mesh for the former and a (6 x 4 x 1) k point mesh for the later. For all cases we have used a vacuum of 12.5Å in the direction perpendicular to plane of the slab.

4.1 Clean Surface

4.1.1 Pt(100)

The change in interplanar distance of the Pt(100) surface after relaxation have been studied with respect to bulk interplanar spacing, using the formula

$$\%\Delta d_{ij} = \frac{d_{ij} - d_{bulk}}{d_{bulk}} \times 100 \tag{4.1}$$

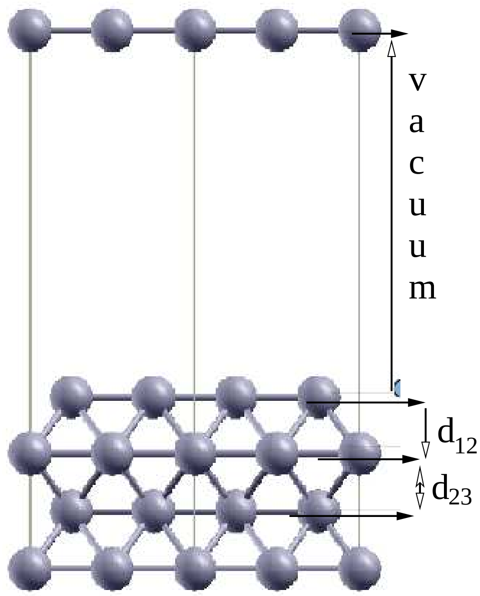

Figure 4.1: Schematic diagram of the layers.

where d_{bulk} is the interplanar distance for bulk Pt and d_{ij} is the interplanar spacing between the ith and jth layer.(See Fig.4.1)

The values of the interplanar spacings are listed in Table 4.1 and are found to

Table 4.1: The change in inter-planar distance for Pt(100) surface.

layer index(ij)	d_{ij} Å	$\%\Delta d_{ij}$ cal.	previous th. cal.	exp
12	1.942	-2.82	-2.6	0.0±5.1
23	1.976	-1.16		

be in excellent agreement with previously calculated values with similar DFT GGA-PBE study -[26] and also experimental measurements. The negative sign in the change in the interplanar spacings indicates a contraction of the layers with respect to the bulk interplanar spacing.

4.1.2 Pt(111)

For Pt(111) the results in the change in interplanar distances are presented in Table 4.2. Our results therein are in good agreement with previous calculations and experimental measurements. The difference observed from the reference [32] is possibly due to the difference in number of layer used to model the slabs and other computational details. We find that unlike Pt(100), for Pt(111) the d_{12} is positive indicating an expansion of the interplanar spacing compared to the bulk Pt. Also the magnitude of the change in d_{ij} in Pt(111) is much smaller compared to Pt(100).

Table 4.2: The change in interplanar distance for Pt(111) surface

layer	$\%\Delta d_{ij}$		
index(ij)	cal.	previous th. cal.	exp.
12	0.67	0.44 [32]	1.1±0.9[32]
23	-0.54	-0.3	

4.2 Adsorption of atomic N and O on Pt surfaces

The adsorption energies for N and O were calculated using the formula:

$$E^{X}_{ads} = E_{M+X} - E_M - E_X \tag{4.2}$$

where E_{M+X}, E_M and E_X are the total energies of the slab and adsorbate X, the energy of the slab, and the energy of the adsorbate in gas phase respectively. M can either be Pt(100) or Pt(111) and X can be either N or O. E_{ads}^{X} is the adsorption energy.

4.2.1 On Pt(100)

Table 4.3 shows the adsorption energy of nitrogen and oxygen on different sites of platinium (100) surface. The different sites considered are represented in the schematic diagram in Fig: 4.2

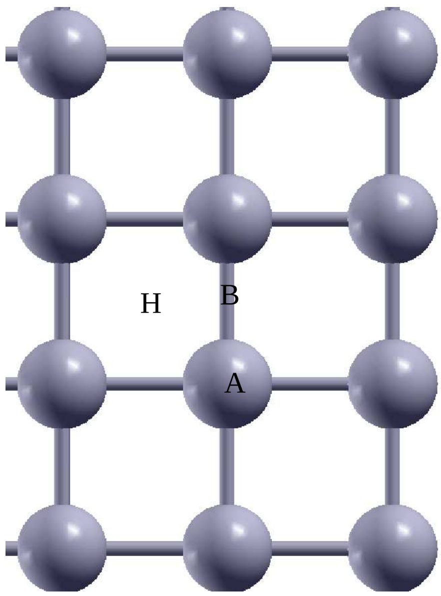

Figure 4.2: Schematic representation of sites for Pt(100). A, B and H is 'atop', 'bridge' and 'hollow' respectively.

For N, the bridge and hollow sites are almost energetically degenerate and they are more preferred compared to the atop site. For O, the bridge site is the most favoured one. The adsorption energies of N and O, reveals that O is more mobile on Pt(100) than N. This is because the change in energy for oxygen in the different sites is lower than the change in energy for nitrogen in the various sites. Adsorption energy of N in the bridge and hollow site are similar, signifying that nitrogen can move easily between these two sites.

Table 4.3: The adsorption energies E^{N}_{ads} for N and O on Pt(100)

Site	E^{N}_{ads}(eV)	E^{O}_{ads}(eV)
atop	-2.41	-3.22
bridge	-4.06	-4.36
hollow	-4.05	-3.92

4.2.2 On Pt(111)

The results of N and O adsorption on Pt(111) are given in Table 4.4. These energies were calculated using eqn. 4.2. The different sites considered are represented in the schematic diagram in Fig: 4.3

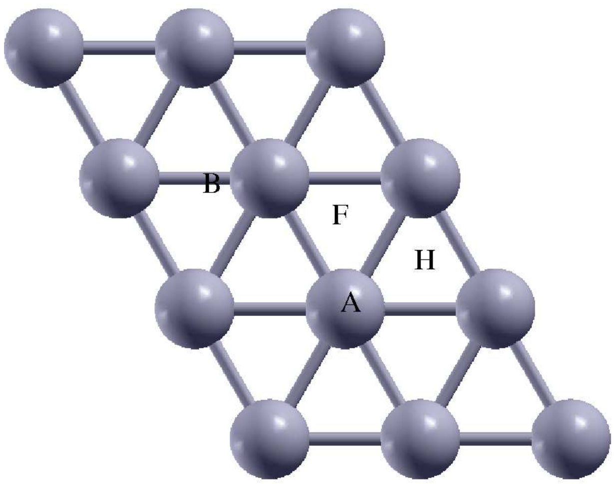

Figure 4.3: Schematic representation of sites for Pt(111). A is 'atop', B is 'bridge', F and H are 'fcc hollow' and 'hcp hollow' respectively.

Table 4.4: The adsorption energies of N and O on Pt(111)

Site	E_{ads}^{N}(eV	$E_{ads}^{O}(eV)$
bridge	-4.50	-4.38
fcc hollow	-4.32	-4.00
hcp hollow	-4.51	-4.38
atop	-4.50	-4.00

For N the bridge, hcp hollow and atop sites are energetically degenerate and are most preferred than the fcc hollow site. For O, the bridge and hcp hollow sites are more preferred than the fcc hollow and atop site. For Pt(100), O is more mobile than N.

4.3 Coadsorption of N and O on Pt surfaces

In order to determine the final state of the NO dissociation reaction we determine the preferred sites for N and O coadsorption on the different surfaces considered in the study. We have calculated the coadsorption energies for cases where N and O are infinitely apart on the surface (corresponding to a hypothetical situation) and when the distance between them are finite. For the former the coadsorption energy is given by:

$$E_{coads}^{\infty} = E_{M:O} + E_{M:N} - 2E_{M} - E_{NO} \tag{4.3}$$

where E_M is the energy of the metal, $E_{M:O}$ and $E_{N:O}$ are the total energies with N and O respectively and E_{NO} is the energy of NO. For the later case, the coadsorption energy is calculated using the following formula

$$E_{coads} = E_{M:N+O} - E_{M} - E_{NO} \tag{4.4}$$

4.3.1 On Pt(100)

The result of E^{∞}_{coad} for different combination of N and O adsorption sites are listed in Table 4.5

Table 4.5: The coadsorption energy at infinite N and O for different site permutation on Pt(100) surface

O	$E^{\infty}_{coad}(eV)$		
Site	N (atop)	N (bridge)	N (hollow)
atop	1.61	-0.04	-0.04
bridge	0.47	-1.18	-1.17
hollow	0.92	-0.73	-0.73

We find two possible situations which are almost energetically degenerate with binding energies of about -1.18eV:

(a) N and O on the bridge sites

(b) N in a hollow site and O on a bridge site.

The other combinations of adsorption sites are much higher in energy (less negative) compared to those mentioned above. Therefore when we study the coadsorption energy of N and O when they are at finite distance apart, we consider only the combinations of the sites (a) and (b). For these calculations, we used a (2x3) unit cell. Within the unit cell we considered different possible combinations of bridge and hollow sites. From the results in the previous section we saw that O is more mobile on Pt(100) compared to N. Therefore, we did the calculations with starting geometries in which N is fixed and O is put in different sites and then relax the top two surface layers together with the N and O atoms. After relaxation we find that while N atom remains on the hollow site the O atoms move to the bridge site.

The adsorption energies are given in Table 4.6 for different geometries. The different sites are shown schematically in Fig. 4.4. The final geometries after relaxation are shown in Fig. 4.5 The geometry 'a' as shown in Fig.4.5, is found to be the lowest in energy.

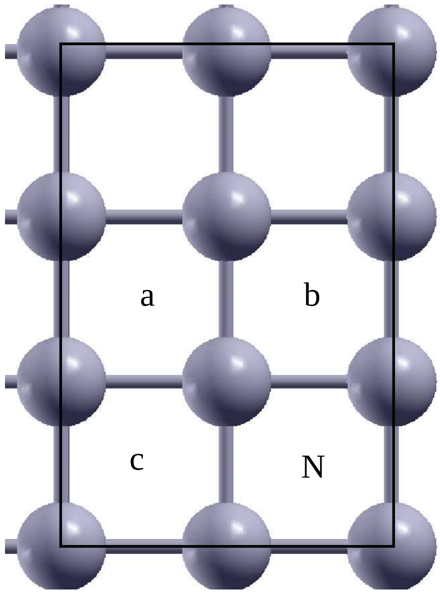

Figure 4.4: Schematic representation of the initial geometry of Table 4.6

For this case, after relaxation, the average interplanar distance between the relaxed top two layers with respect to both the bulk interplanar separation and that of the clean surface. However, the interplanar separation between the 2^{nd} and 3^{rd} layers is same as that of bulk. A graph of adsorption energy versus the inverse of the distance between N and O was plotted for the system in Fig. 4.6. As N and O comes closer E_{coads} decreases which indicates a repulsive interaction between N and O on this surface when they are in their atomic form.

Table 4.6: Coadsorption energies (E_{coads}), change in interplanar distances($\%d_{ij}$), Pt-N distance(d_{Pt-N}), Pt-O distance (d_{Pt-O}) and N-O distance(d_{N-O}) for N and O coadsorption on Pt(100) surfaces The numbers in the bracket beside the values of d_{Pt-N} indicates the number of each bonds

Sites	E_{coads} (eV)	$\%\Delta d_{12}$	$\%\Delta d_{23}$	d_{Pt-N} (Å)	d_{Pt-N} (Å)	d_{N-O} (Å)
a	-1.18	1.28	0.00	2.02 (4)	1.96 (2)	5.13
b	-1.17	1.35	-0.66	2.12(2) 2.11 (2)	1.96 (2)	4.28
c	-0.45	3.07	-0.65	2.12 (2) 2.07 (2)	1.96 (2)	3.65

4.3.2 On Pt(111)

The result of the calculation of coadsorption energy of N and O when they are infinitely apart on Pt(111) is tabulated in Table 4.7. From Table 4.7, the combination of N on the bridge, hcp hollow and atop sites and O on the bridge and hcp sites are found to be degenerate in energy and the coadsorption energy being about -1.64eV. The other combinations are of higher energy.

Now we study the coadsorption energy of N and O at finite distances apart. We consider the combinations of sites for which oxygen is at the bridge and hcp hollow sites and N at different bridge, hcp hollow and atop sites as shown in Table 4.8 (see Fig.4.7 fpr a schematic representation of the sites). The top two layers of these geometries together with the N and O atoms were relaxed and their adsorption energies calculated applying eqn.4.4. For the

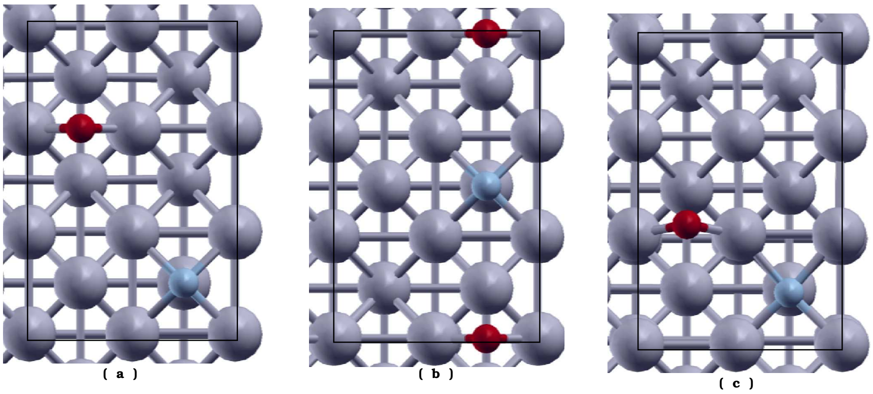

Figure 4.5: Coadsorption geometries at N and O adsorbed on Pt(100). Oxygen is denoted by red circle, Nitrogen by blue circle and Platinium by grey circles

case in which the O atom was on the bridge site in their initial conditions, we find that after relaxation it moves either to hcp hollow of fcc hollow site.

Fig. 4.9 represents the relaxed geometries and the corresponding values for coadsorption energy is given in Table 4.9. Geometries ‘a’ and ‘b’ are energetically degenerate and lowest in energy. To study the behaviour of the coadsorption energies as a function of the distances between N and O in the (2x3)unit cell we have plotted for systems that have O in the hcp site and N in the fcc site as their final geometry. This curve is shown in the Fig. 4.8.

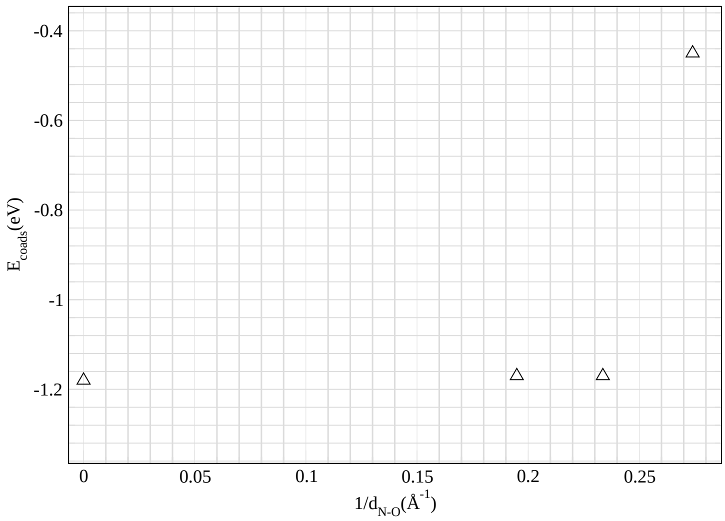

Figure 4.6: Coadsorption energy versus $\frac{1}{d_{N-O}}(Å^{-1})$ for Pt(100)

Table 4.7: The adsorption energy at infinite N and O for different site permutation on Pt(111) surface.

O Sites	E_{ads}(eV)			
	N (bridge)	N (fcc)	N (hcp)	N (atop)
bridge	-1.64	-1.46	-1.64	-1.64
fcc	-1.26	-1.08	-1.26	-1.26
hcp	-1.64	-1.46	-1.65	-1.64
atop	-1.26	-1.08	-1.27	-1.26

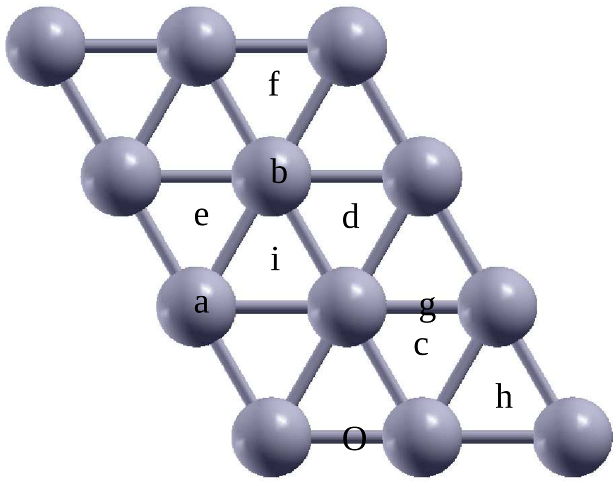

Figure 4.7: Schematic representation of Table4.8

Table 4.8: Initial Geometry for table(4.9), Oxygen is kept in the bridge site.(Fig.4.7)

	Nitrogen			
	atop	fcc	bridge	hcp
O		c	g	h
	a	d		
	b	e		i
		f		

Table 4.9: Coadsorption energy for Pt with N and O in the (2x3) unit cell

Sites	O	E_{coad}(eV)		
		N (fcc)	N (hcp)	d_{N-O} Å
a	hcp	-1.28		4.30
b	hcp	-1.28		3.78
c	fcc	-0.77		3.07
d	hcp	-1.03		3.47
e	hcp	-1.28		3.56
f	hcp	-0.79		3.39
g	hcp	-1.27		3.05
h	hcp		-1.02	2.83
i	hcp		-1.32	3.05

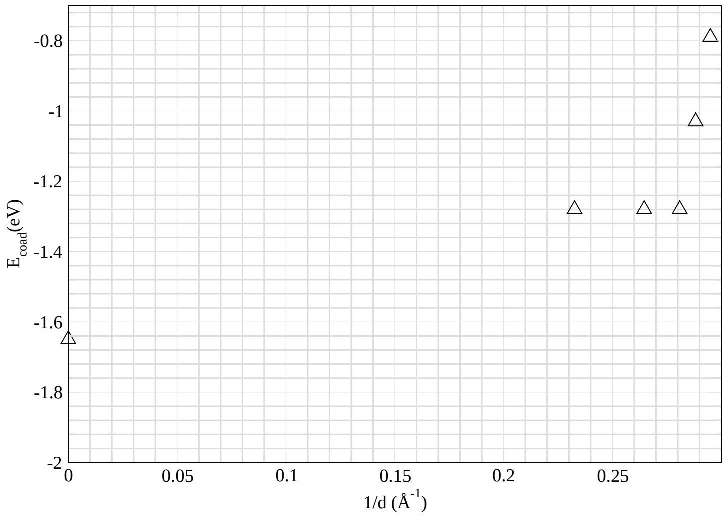

Figure 4.8: E_{coads}(eV) vs. $\frac{1}{d}$(Å^{-1})

Table 4.10: Initial geometry considered by us keeping oxygen on the hcp hollow site

	atop	fcc	bridge	hcp
O	C	E	D	A
		F		B
		G		

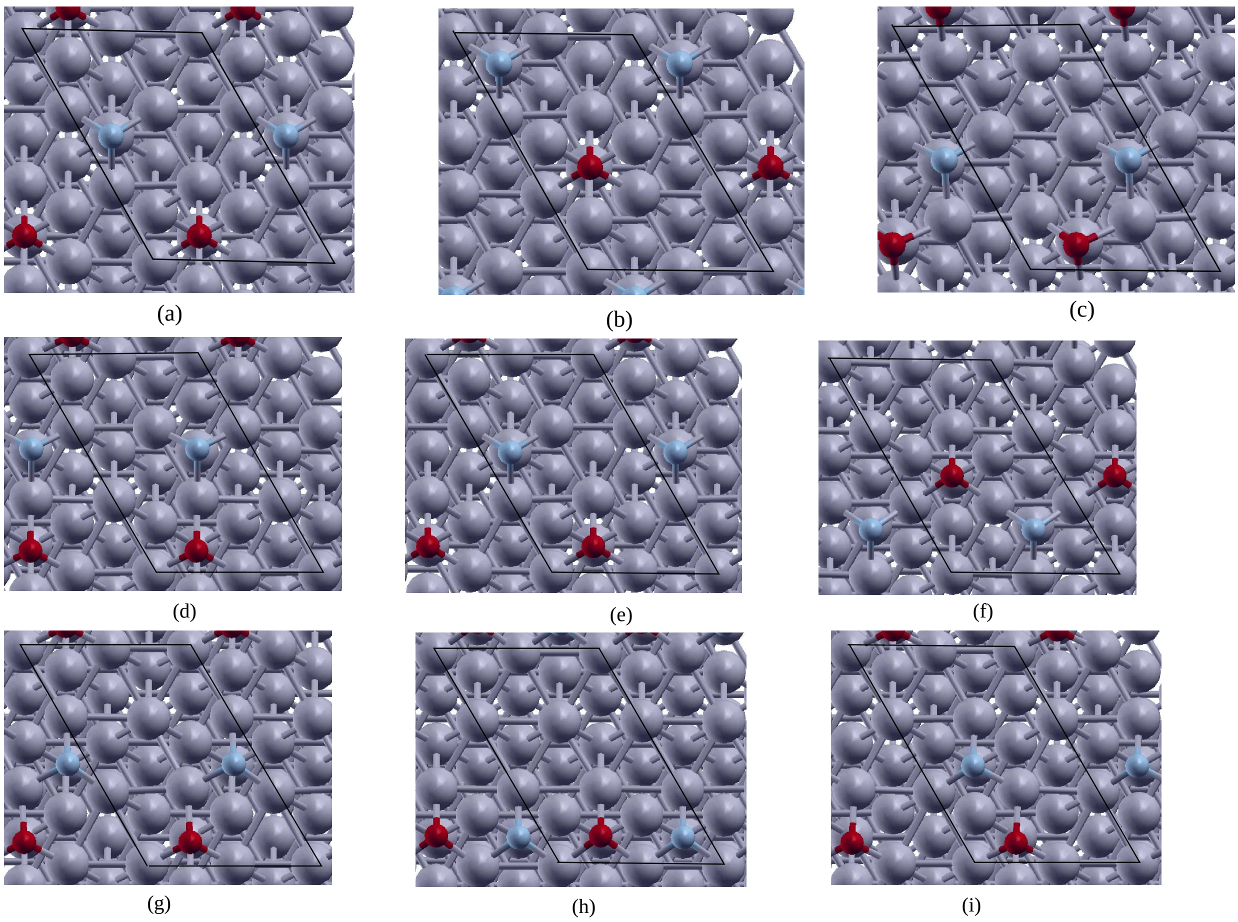

Figure 4.9: Geometry after relaxation of i.e table(4.9), Red = O, Blue = N, and Grey = Pt

Chapter 5

Conclusion

In this work we have determined the N and O coadsorption geometries and energies on Pt(100) and Pt(111) surfaces; N and O coadsorbed on these surfaces correspond to the final state of the reaction:

$$NO_{(a)} \longrightarrow N_{(a)} + O_{(a)}$$

where the subscript 'a' denotes that NO, N and O are bound to the catalyst. The above reaction is the rate limiting step for conversion of NO to less harmful products.

In achieving this aim, firstly, we studied the adsorption of N and O on Pt(111) and Pt(100) surfaces, of which we calculated their adsorption energies in order to determine which is more mobile on the different surfaces. We found that on Pt(100) surface, O is more mobile than N, and for the Pt(111) surfaces both of them have similar mobility.

We also studied the coadsorption energies of N and O for different adsorption geometries and also as a function of the distance between N and O on the two above mentioned surfaces.

On Pt(100), among the geometries considered by us, we find N prefers to stay on a hollow site and O at a bridge site of 5.13 Å away from N. The study of the variation of coadsorption energy with the distance between N and O in their atomic form on Pt(100) is repulsive in nature.

On Pt(111), we find that there are several possible coadsorption geometries which may be prefered by N and O on this surfaces.

With the help of the above results obtained in our study and with the information about the initial state of the reaction, i.e., the adsorption geometries of NO in molecular form on these surfaces, it will be possible to calculate the barrier for the NO dissociation on these surfaces.

Bibliography

[1] I.E. Erikat, B.A Hamad, and J.M. Khalifeh, Phys. J.B 67, 35 - 41, 2009.

[2] Raghani Pushapa, and Prasenjit Ghosh, Shobhana Narasimhan, and Stefano de Gironcoli "Effective coordination as a predictor of adsorption energies: A model study of NO on Rh(100) and Rh/MgO(100)surfaces.",(2009).

[3] P. Ghosh, R. Pushpa et. al "Effective coordination number: a simple indicator of activation energies for NO dissociation on Rh(100) surfaces,

[4] W. Kohn and L. J. Sham. Phys.Rev, 140:A1133, 1965

[5] "Physics at Surfaces",Andrew Zangwill, Cambridge University Press, N.Y (1988).

[6] "Density-Functional Theory of Atoms and Molecules." Oxford Science Publications (1989).

[7] C, Herring, Phys.Rev 57 (1940) 1169.

[8] GGA pseudo-potential is taking from http://www.quantum-espresso.org/pseudo.php

[9] PI J.C. Phillips and L. Kleinman, Phys. Rev. 116 287, 1959.

[10] D. Vanderbil. Phys. Rev. B, 41:7892, 1990.

[11] A. Baldereschi. Phys. Rev. B, 7:5212, 1973.

[12] Dario Alf." First Principles Study of Two Rhodium Surfaces upon Carbon Monoxide and Oxygen Adsorption." PhD thesis, Scuola Internazionale Superiore di Studi Avanzati - SISSA, 1997.

[13] D. Ceperley and B. Alder. Phys. Rev. Lett., 45:566, 1980.

[14] R. Pushpa, P. Ghosh, S. Narasimhan, and S. de Gironcoli. Effective coordination as a predictor of adsorption energies: A model study of NO on Rh(100) and Rh/MgO(100) surfaces. , 79(16):165406, April 2009.

[15] J. P. Perdew and A. Zunger. Phys. Rev. Lett., B23:5040, 1981.

[16] J. P. Perdew and Y. Wang Phys. Rev. B 45, 13244, 1992.

[17] J. P. Perdew, J. A. Chevary, S. Vosko, K. A. Jackson, M. R. Pederson, D. J. Singh, and C. Fiolhais Phys. Rev. B 46, 6671 (1992).

[18] H. J. Monkhorst and J. D. Pack. Phys. Rev. B, 13:5188, 1976.

[19] R. P. Feynman,"Forces in Molecules". Phys. Rev. 56 (4): 340. doi:10.1103/PhysRev.56.340, 1939

[20] M. Schluter D. R. Hamann and C. Chiang. Phys. Rev. Lett., 43(1979), 1994.

[21] H. Hellmann."Einfhrung in die Quantenchemie" Leipzig: Franz Deuticke. p. 285, 1937

[22] P. Giannozzi, S. Baroni, N. Bonini, M. Calandra, R. Car, C. Cavazzoni, D. Ceresoli, G. L. Chiarotti, M. Cococcioni, I. Dabo, A. Dal Corso, S. Fabris, G. Fratesi, S. de Gironcoli, R. Gebauer, U. Gerstmann, C. Gougoussis, A. Kokalj, M. Lazzeri, L. Martin-Samos, N. Marzari, F. Mauri, R. Mazzarello, S. Paolini, A. Pasquarello, L. Paulatto, C. Sbraccia, S. Scandolo, G. Sclauzero, A. P. Seitsonen, A. Smogunov, P. Umari, and R. M. Wentzcovitch. Quantum espresso: a modular and open-source software project for quantum simulations of materials, 2009.

[23] D. J. Chadi and M. L. Cohen. Phys. Rev. B, 8:5747, 1973.

[24] C. L. Fu and K. M. Ho. Phys. Rev. B, 40:5480, 1983.

[25] H. Knzinger, K. Kochloefl Heterogeneous Catalysis and Solid Catalysts in Ullmann's Encyclopedia of Industrial Chemistry, Wiley-VCH, Weinheim. 2002.

[26] Hairong Tang and Berhardt L. Trout. NO Chemisorption on Pt(111), and Pd/Pt(111). J.Phys.Chem. B, 109:1763017634, 2005.

[27] B.A. Hamad I.A. Erikat and J.M. Khalifeh. Adsorption of O and CO on Ir(100) from first principles. Euro.Phys.J.B, 67:3541, 2009.

[28] B. Hammer and J. K. Norskov. Theoretical surface science and catalysis. Phys.Rev. B, 72:205419, 2005.

[29] F.D. Murnaghan, Proc. Natl. Acad. Sci. USA **30**, 244 1944.

[30] Z Zhao, L. Wang, J.Mega, Phys. Rev. B **73**, 193309, 2006.

[31] "Infrared and Raman Spectra of Inorganic and Coordination Compounds." New York: Wiley, 4th edition, 1986.

[32] Peter J. Feibelman. First-principle calculations of stress induced by gas adsorption on Pt(111). Phys.Rev. B, 56(4):2175, 1997.